Barry S. Siegal
Michael J. Abrams
Jet Propulsion Laboratory
Pasadena, CA 91103

Geologic Mapping Using LANDSAT Data

The range of wavelength bands sensed by LANDSAT were found to be unsatisfactory in a test of several algorithms for automated lithologic classification.

INTRODUCTION

THE SUCCESSFUL LANDSAT missions have provided the scientific community with vast quantities of new data about the earth. For the geologist, the synoptic view provided by satellite imagery has proved especially useful. Of additional value is the mul-

32,000 km², is acquired in the four spectral bands by the MSS. Each scene contains over 3×10^7 bits of information, representing the reflected brightness values (DN) of each pixel in each wavelength band.

This is far more data than can be meaningfully displayed in one image. Therefore, one

ABSTRACT: *The feasibility of automated classification for lithologic mapping with LANDSAT digital data was evaluated by using three classification algorithms. The two supervised algorithms analyzed, a linear discriminant analysis algorithm and a hybrid algorithm which incorporated the Parallelepiped algorithm and the Bayesian maximum likelihood function, were comparable in terms of accuracy; however, classification was only 50 per cent accurate. The linear discriminant analysis algorithm was three times as efficient as the hybrid approach. The unsupervised classification technique, which incorporated the CLUS algorithm, delineated the major lithologic boundaries and, in general, correctly classified the most prominent geologic units. The unsupervised algorithm was not as efficient nor as accurate as the supervised algorithms. The inability of all the classification schemes to portray correctly the lithologic units reflects the inhomogeneity of the geologic units and the similarity of their spectral signatures in the wavelength bands measured by LAND-SAT. Analysis of spectral data for the lithologic units in the 0.4 to 2.5 μm region, as obtained by a portable field reflectance spectrometer, indicated that a greater separability could be obtained using wavelength bands outside the region sensed by LANDSAT.*

tispectral information obtained for each scene by the satellite's multi-spectral scanner (MSS). This scanner simultaneously sensed the ground in four spectral bands, 0.5 - 0.6 μm (band 4), 0.6 - 0.7 μm (band 5), 0.7 - 0.8 μm (band 6), and 0.8 - 1.1 μm (band 7), with a resolution element (pixel) size of 59 × 79 meters. One LANDSAT scene, about

major problem facing the user is how best to display and analyze this data. One solution is to display only that subset of the data which is useful to the analyst. Because the data are acquired in digital form, a digital computer can be used to handle what would otherwise be an unmanageable amount of information.

Basically, two techniques have been de-

PHOTOGRAMMETRIC ENGINEERING AND REMOTE SENSING,
Vol. 42, No. 3, March 1976, pp. 325-337.

325

veloped and used for computer processing of this data: enhancement and classification. Enhancement procedures (Goetz *et al.*, 1975) attempt only to optimize the display of some particular feature or parameter implicit or explicit in the image. Various methods used include contrast stretching, spatial filtering, and band-to-band ratioing. The last method is particularly useful since, to the first order, it removes the variations of albedo due to topography, and gives a truer picture of the spectral characteristic of a material by describing the slope of the spectral curve (Rowan *et al.*, 1974).

Classification procedures seek to interpret an image in terms meaningful to the user. They have been successfully applied in the fields of agriculture (Draeger *et al.*, 1973; Wigton and Von Steen, 1973; Bauer and Cipra, 1973) and land use (Anderson *et al.*, 1972; Ellefsen *et al.*, 1973). In the field of geology, classification routines, in general, have not been so successful. This is primarily due to the inhomogeneity of geologic units, presence of gradational boundaries, confusing influence of both vegetative cover and soil mantling, and similarity of the spectral signature of different lithologies. These problems are absent or not so pronounced in remote sensing studies in land use or agriculture.

Although some investigators (for example, see Melhorn and Sinnock, 1973) have applied one particular classification scheme to the problem of lithologic identification, a comparison of different techniques applied to the same area has not been reported. This paper presents the results of a recent study using three different classification techniques applied to the problem of geologic mapping. The techniques analyzed were a hybrid classifier, which is a modification of Purdue's LARSYS: CLUS, an iterative unsupervised classifier which provides optimum natural classification; and a linear discriminant analysis algorithm. The relative success of the schemes are evaluated by comparison with the known geology of the study region, and by analysis of the reflectance spectra of representative samples of each geologic unit as determined in the field.

CLASSIFICATION

Classification is the process of recognizing classes or groups whose members have certain characteristics in common. Ideally, the classes should be mutually exclusive and exhaustive; that is, there should be one and only one class to which an element is assigned, and all elements in the domain of

interest may be so assigned. In practice, these requirements are difficult to fulfill and often are not achieved (Griffiths, 1968).

The classes or groups are based on properties possessed by the elements of a population, and classes are formed by grouping together those elements of a population that are alike, where likeness is defined by certain selected properties or criteria (Griffiths, 1968; Block, 1972). An optimum classification will group elements together into classes which are separated from one another by discontinuities in the ranges of their observed properties (Imbrie and Purdy, 1962).

Classifications can be either natural or artificial. In a natural classification, not only are the classes mutually exclusive and exhaustive, but they are based on the essential characteristics of the elements under investigation, and those elements are grouped together which possess fundamental similarities. In an artificial classification, the grouping is determined by superficial resemblances or external criteria. The boundaries between the groups are artificial even though they may have been objectively determined (Hempel, 1952; Imbrie and Purdy, 1962).

In general, most classification schemes used for LANDSAT data are artificial. Analysts are concerned with classifying LANDSAT images into various subsets, each corresponding to features or themes of specific interest, such as geologic units, soils, cultural features or vegetation. Two different approaches to classification of LANDSAT imagery are generally used. The classification can be supervised, in which training areas are established by the analyst, or unsupervised in which the boundaries are objectively determined from a computer algorithm to delineate natural clusters. In supervised classification, each training area, which supposedly is representative of a specific feature of interest, is determined from *a priori* knowledge, i.e., "ground truth." Statistics are computed for each theme and are used in various automated techniques to identify other areas within the LANDSAT image which have similar characteristics. In unsupervised classification, no *a priori* knowledge is assumed, and the classes are based on the actual relations among the variables. In such classification schemes the number of classes can be established by the analyst or, more objectively, through the use of an algorithm in which the data itself is used to suggest the number of natural categories; that is, to find the number of clusters.

CLASSIFICATION TECHNIQUES ANALYZED

UNSUPERVISED APPROACH (CLUS)

The unsupervised classification scheme considered here, CLUS, is an iterative technique (Rubin and Friedman, 1967) in which the "best" partition of n objects into g groups is based on evaluation of variance and covariance matrices.

The Rubin and Friedman method is applicable to the general problem of classification even when the number of groups is unknown. The algorithm followed is one in which the data itself (p measurements on n objects) is used to suggest "natural categories"; that is, to find the clusters.

The best partition of n objects into g groups is defined as that partition, out of all possible partitions of the objects into g groups, for which a numerical valued criterion function achieves its maximum value. Several criterion functions exist in the CLUS program. They all depend on the fundamental relationship $T = W + B$, where W is the pooled within-group matrix of cross products of deviations, T is the matrix of cross products of deviations for the total sample, and B is the matrix of cross products of deviations of groups from the grand means weighted by group size (Cooley and Lohnes, 1962). The elements of each of the matrices are

$$w_{ij} = \sum_{k=1}^{g} \sum_{n=1}^{n_g} (X_{ikn} - \overline{X}_{ik})\ (X_{jkn} - \overline{X}_{jk})$$

$$t_{ij} = \sum_{n=1}^{n} (X_{in} - \overline{X}_i)\ (X_{jn} - \overline{X}_j)$$

$$b_{ij} = \sum_{k=1}^{g} n_g (\overline{X}_{ik} - \overline{X}_i)\ (\overline{X}_{jk} - \overline{X}_j)$$

where g is the number of groups, n_g is the number of objects in group g, X_{ikn} is the measurement, for variable i, on the nth object in group k, n is total number of objects; and i and j run from 1 to p, the number of variables. The "best" classification is the one which maximizes the between-group and minimizes the within-group variation.

The CLUS algorithm includes five criteria which may be used to determine the "best" classification (see Siegal and Griffiths, 1975). One criterion function is the logarithm of the ratio between the determinant of T and B ($\log |T| / |B|$) where $T/B = 1 + W$ so that maximizing $\log |T| / |B|$ is the requirement. The value of this criterion function may be used as an informal indicator of the best

number of groups by examining its change in value as the number of groups is increased (Rubin and Friedman, 1967).

A second criterion uses Mahalonobis D^2, a multi-dimensional Euclidean distance function in which the distance between groups is compared with the distance within groups; the aim is to maximize variation between groups as compared with the distance within groups.

A third procedure examines the trace of W (Tr. W) and attempts to minimize this function (i.e., minimize the sum of squares within groups).

The other two criteria are approximations to $\log |T| / |B|$ and to Mahalonobis D^2.

The CLUS algorithm also contains routines for improving the initial grouping; for example, it is possible to apply or suppress hill-climbing routines, forcing passes, and reassignment passes (Rubin and Friedman, 1967). One may also start from a single group (the conjoint partition of Rubin and Friedman, 1967), from a chosen or previously obtained grouping, or from a random start (see Griffiths, 1970). Finally, after achieving an optimal grouping, it is possible to establish a key by using linear discriminant functions which may be used to assign additional samples to one of the established classes.

Although iterative unsupervised classification techniques such as CLUS provide an optimum classification, these procedures are time consuming and require large amounts of computer core. Classification of LANDSAT data by such algorithms must therefore be based initially on the classification of a random, representative, small sample of the population under study.

SUPERVISED APPROACH

In a supervised classification scheme, at least one training area must be defined for each class or theme. The training areas should be representative of the classes to be investigated and consist of a subset of the original data in p–dimensional space, where each dimension is a spectral band or ratio of bands. (As noted earlier, the use of ratios describes the slope of the spectral curve and gives a truer picture of the spectral character of a material.) The two classification schemes considered here are linear discriminant analysis and a hybrid approach which incorporates a parallelepiped algorithm and the Bayesian maximum likelihood function.

Linear Discriminant Analysis. Discriminant function analysis consists of finding a

transform which minimizes the ratio of the difference between group multivariate means to the group multivariate variances.

The algorithm used here (after UCLA BMDO7M Program) computes a classification function for each of the themes by choosing and inputting the independent variables in a stepwise manner. The variable entered at each step is selected on the basis of its F statistic. At each step of the analysis a classification function is computed for each theme. The equation of the classification function D_{ki} for the kth theme for the ith variable is given by

$$D_{ki} = c_{ko} + \sum_{i=1}^{r} e_{ki} z_{lki}$$

where c_{ko} is the constant term for the kth theme, r is the number of input variables (spectral bands or ratios), e_{ki} is the discriminant coefficient for the kth theme and the ith variable, and z_{lki} is the measured spectral parameter of the lth case of the kth theme for the ith variable.

The constant term c_{ko} is computed from $-1/2 \sum_{i=1}^{r} e_{ki} \bar{X}_{ki}$, where $\bar{X}_{ki}$ is the mean of variable i for theme k. The coefficient e_{ki} is computed from $(n-g) \sum_{j=1}^{r} \bar{X}_{kj} a_{ij}$. At each step of the procedure the variables are divided into two disjoint sets: those included in the discriminant functions (r) and those not included. The within-group matrix of cross products of deviations (W) and the matrix of cross products of deviations for the total sample (T) are computed as previously described. The W and T matrices are partitioned into

$$W = \begin{bmatrix} W_{11} & W_{12} \\ W_{21} & W_{22} \end{bmatrix} \quad T = \begin{bmatrix} T_{11} & T_{12} \\ T_{21} & T_{22} \end{bmatrix}$$

where W_{11} and T_{11} are $r \times r$, and r is the number of variables included in the discriminant functions.

The elements a_{ij} are derived from matrix A, and the elements b_{ij} from matrix B:

$$A = \begin{bmatrix} W_{11}^{-1} & W_{11}^{-1} W_{12} \\ W_{21} W_{11}^{-1} & W_{22} - W_{21} W_{11}^{-1} W_{12} \end{bmatrix} = \{a_{ij}\}$$

$$B = \begin{bmatrix} T_{11}^{-1} & T_{11}^{-1} T_{12} \\ T_{21} T_{11}^{-1} & T_{22} - T_{21} T_{11}^{-1} T_{12} \end{bmatrix} = \{b_{ij}\}$$

The optimum input variables (spectral channels or ratios) are chosen on the basis of

the largest F-statistic, where, for the entry of the jth variable.

$$F_j = \frac{a_{jj} - b_{jj}}{b_{jj}} \cdot \frac{n-r-g+1}{g-1}$$

where n is the total number of cases and g is the number of themes. The degrees of freedom are $g-1$ and $n-r-g+1$. An iterative technique is used to determine the best linear combination of spectral bands (or ratios).

Hybrid Approach. The hybrid classification technique combines two existing classification schemes, the Parallelepiped algorithm and the Bayesian maximum likelihood function (Addington, 1975). In this classification scheme, the means and covariance matrix are computed for each theme specified, assuming Gaussian distributions. These statistics define the themes; the number of standard deviations about the mean can be specified by the analyst to represent the ideal decision boundaries for each class. In p-dimensional space, these decision boundaries are hyperellipsoids. The Parallelepiped algorithm approximates the hyperellipsoids with hyperrectangles. If an unknown pixel falls within one of the hyperrectangles, it is assigned to that class; if it does not fall within one of them, it is considered unknown; and if it falls into an area where hyperrectangles overlap, it is considered ambiguous.

Computationally (Addington, 1975), each picture element (pixel) of the multi-spectral imagery data is considered as the transpose of a p-dimensional vector $X^T (X_1 \, X_2 \ldots X_p)^T$, where p is the number of spectral bands. The mean and standard deviation of the jth class out of a possible m classes are μ and $\hat{\sigma}_j$, respectively. The Parallelepiped algorithm assigns a pixel to class j_o if and only if $\mu_{i,j_o} - \delta\hat{\sigma}_{i,j_o} \leq X_i \leq \mu_{i,j_o} + \delta\hat{\sigma}_{i,j_o}$ for each $i = 1, 2, \ldots, p$ and δ = constant defining the confidence interval.

The Bayesian algorithm is used to resolve ambiguities or to assign unknowns which arise through use of the Parallelepiped algorithm. In the former case, the statistical likelihood that a pixel falls into each of the ambiguous classes is computed; in the latter, the likelihood for all classes is computed. The class with the maximum likelihood is then chosen as the class to which the pixel is assigned. The likelihood of $\bar{X}^T$ being a member of class j is defined by the normal multivariate probability density function P_j, where

$$P_j = \frac{1}{(2\pi)^{p/2} k_j^{1/2}} \cdot$$

$$\exp\left\{-1/2 \left(X - \overline{\mu}_j\right)^T K_j^{-1} \left(X - \overline{\mu}_j\right)\right\}$$

where K_j is the covariance matrix $(p \times p)$ of the jth class and $K_j = \det(K_j)$. In practice, it is not P_j which is computed, but $\ln P_j$. This is appropriate since $\ln$ is a monotonic increasing function and only the maximum P_j is desired.

STUDY AREA AND TRAINING AREAS

The 20-by-20 km study area (200-by-300 pixels on the LANDSAT image) is located in the Coconino Plateau in north central Arizona (see Figure 1). The Plateau has been geologically mapped in detail (Goetz *et al.*, 1975) and consists of a stripped Miocene surface formed on the Permian Kaibab Formation. This formation has been subdivided into five mappable units: the oldest unit, unit Beta, consists of a thick sequence of gray dolomitic limestones, with minor thin chert beds; unit 2 is a 5-10 m thick yellow dolomitic limestone; unit 3 is a 10 m thick red-brown sandstone and siltstone bed; unit 4-5 consists of a yellow dolomitic limestone overlain by red-brown shale and siltstone; and unit 6 is a yellow-gray dolomitic limestone, 5-10 m thick. The Moenkopi Formation (TRM) overlies the Kaibab Formation and consists of red siltstone and sandstone (see Plate 1a). Topography is generally subdued except where Cataract Creek has formed precipitous canyons, with relief of 1200 m or more. Vegetation is sparse to moderate and consists of grasses and scrub brushes.

FIG. 1. Location map of the study area.

Training areas for the supervised classification algorithms were chosen from within the study area. For each of the five subdivisions of the Kaibab Formation, two training areas were used; only one area was used for the Moenkopi Formation because of its limited outcrop area in the study region. Each training area covered 25 pixels and its size and location were selected on the basis of large areal extent of the unit, homogeneity as determined from examination of LANDSAT imagery, and minimal but not insignificant soil covering. The spectral radiance of the individual pixels in the LANDSAT MSS bands was extracted for each training area. Ratios of MSS spectral bands (4/5, 4/6, 4/7, 5/6, 5/7, 6/7) were computed and used with the raw spectral values as variables in the classification schemes.

ANALYTICAL APPROACH
UNSUPERVISED CLASSIFICATION (CLUS)

The reflected brightness values (DN) for every nineteenth line and sample of the study area were extracted and ratioed, yielding a 361 × 10 data matrix $(n \times p)$. As would be expected if different groups are present, the univariate frequency distributions are polymodal.

The data matrix was transformed to the equivalent $(p \times p)$ correlation matrix (Table 1) in which all means are zero and variances are unity $(\overline{X}_j = 0, \hat{\sigma}_j^2 = 1)$, thus removing the effects of different scales of measurement.

The correlation matrix was transformed to a components matrix, C_{ij} (see Table 2). This procedure enables the determination of the number of linearly independent sources of information which occur in the matrix of observations; i.e., the rank of the matrix. The extracted components are orthogonal to each other, thus statistically independent. Each component is expressed as some linear combination of the variables, where each variable has a specific factor loading (Dahlberg and Griffiths, 1967).

The rotated matrix of factor loadings is given in Table 2. The first factor is heavily loaded on the MSS ratios 4/5, 4/6, 4/7 and accounts for over 31 per cent of all the information in the original data matrix. The second factor accounts for an additional 31 per cent and is heavily loaded on MSS bands 5, 6, and 7. The third factor explains an additional 18 per cent and is loaded primarily on the MSS ratio 6/7. The remaining 19 per cent of the variation of the original data matrix is accounted for by the fourth component which is heavily loaded on the MSS ratio 5/7,

TABLE 1. CORRELATION MATRIX[1]

	MSS	4	5	6	7	4/5	4/6	4/7	5/6	5/7	6/7
MSS	4	1.00									
	5	0.62	1.00								
	6	0.51	0.79	1.00							
	7	0.51	0.83	0.83	1.00						
	4/5	0.48	0.37	0.27	0.31	1.00					
	4/6	0.55	0.11	0.42	0.25	0.78	1.00				
	4/7	0.58	0.11	0.23	0.38	0.82	0.84	1.00			
	5/6	0.19	0.35	0.27	—	0.15	0.48	0.18	1.00		
	5/7	0.24	0.39	—	0.17	0.13	0.23	0.43	0.57	1.00	
	6/7	—	—	0.35	0.21	—	0.30	0.23	0.53	0.36	1.00

[1] Correlation less than 0.110 omitted (criterion r_{ij} for 300 df = 0.113 at the 5 per cent level)

TABLE 2. ROTATED MATRIX OF FACTOR LOADINGS[1] $[k \times p, p = 10, k = 4)$

		C_1	C_2	C_3	C_4	Comm.
MSS	4	0.69	0.70	—	−0.13	0.99
	5	—	0.91	—	−0.38	0.99
	6	−0.17	0.91	−0.37	—	0.99
	7	−0.18	0.95	0.20	0.16	0.99
	4/5	0.94	−0.18	—	0.26	0.99
	4/6	0.89	−0.13	0.36	−0.22	0.99
	4/7	0.92	−0.13	−0.17	−0.30	0.99
	5/6	—	—	0.66	−0.74	0.99
	5/7	0.12	—	−0.22	−0.97	0.99
	6/7	—	—	−0.99	−0.15	0.99
Eigenvalues		3.11	3.13	1.80	1.90	
Variation exp.		31.16	31.30	18.04	19.05	
Cumulative %		31.16	62.46	80.50	99.56	

[1] Loadings less than 0.110 omitted (criterion r_{ij} for 300 df = 0.113 at the 5 per cent level)

with a secondary loading on MSS ratio 5/6. As expected and as indicated by the communalities (h^2 = 1.00), the four components account for all the variations in the variables

The loadings of the first two factors of the principal component analysis reflect: (1) the strong interrelationship of three of the original variables (MSS bands 5, 6, 7) and (2) the orthogonality and interrelationship of their ratios with MSS band 4. The apparent "independence" of MSS ratios 6/7 and 5/7 with respect to each other and with respect to the first two factors also reflects the effects induced by ratioing correlated data. Nevertheless, as noted earlier, the use of ratios describes the slope of the spectral curve of a material's surface, and is independent of albedo. Although different materials may have similar MSS DN values due to the unevenness of illumination intensity caused by topography, the ratios of their MSS bands would be different, and hence the materials should be separable.

Classification using the CLUS procedure (Rubin and Friedman, 1967) was performed for 2, 3, 4, 5, 6, and 7 groups, according to the following program specifications:

(1) the criterion maximized was the logarithm of the ratio of the determinant of the total variation to the determinant of the variation within groups (i.e., log ($|T| / |W|$));

(2) principal components were not taken, and the input variables (MSS bands 4, 5 and ratios 4/6, 5/6 and 6/7) were chosen on the basis of the principal component analysis of the ten variable data sets and were standardized with mean 0 and variance 1; and

(3) several alternative options were used to achieve an optimum classification.

Over 130,000 partitions of the data were evaluated. The partitioning criterion functions for the best partitions of the data into 2, 3, 4, 5, 6, and 7 groups are tabulated in Table 3. The value of the criterion log ($|T| / |W|$) increases over the 2-to-7 group range with a maximum difference between groups 2 and 3. Similarly, with the Mahalanobis D^2 criterion the largest difference occurs between 2 and 3 groups. This difference is considered to be significant, suggesting an optimum

MOENKOPI
FORMATION

UNCONFORMITY

KAIBAB FORMATION

UNIT 6

UNITS 4 & 5

UNIT 3

UNITS 1 & 2

UNIT β

OLDER
PALEOZOICS

A

B

0   5   10
KILOMETERS

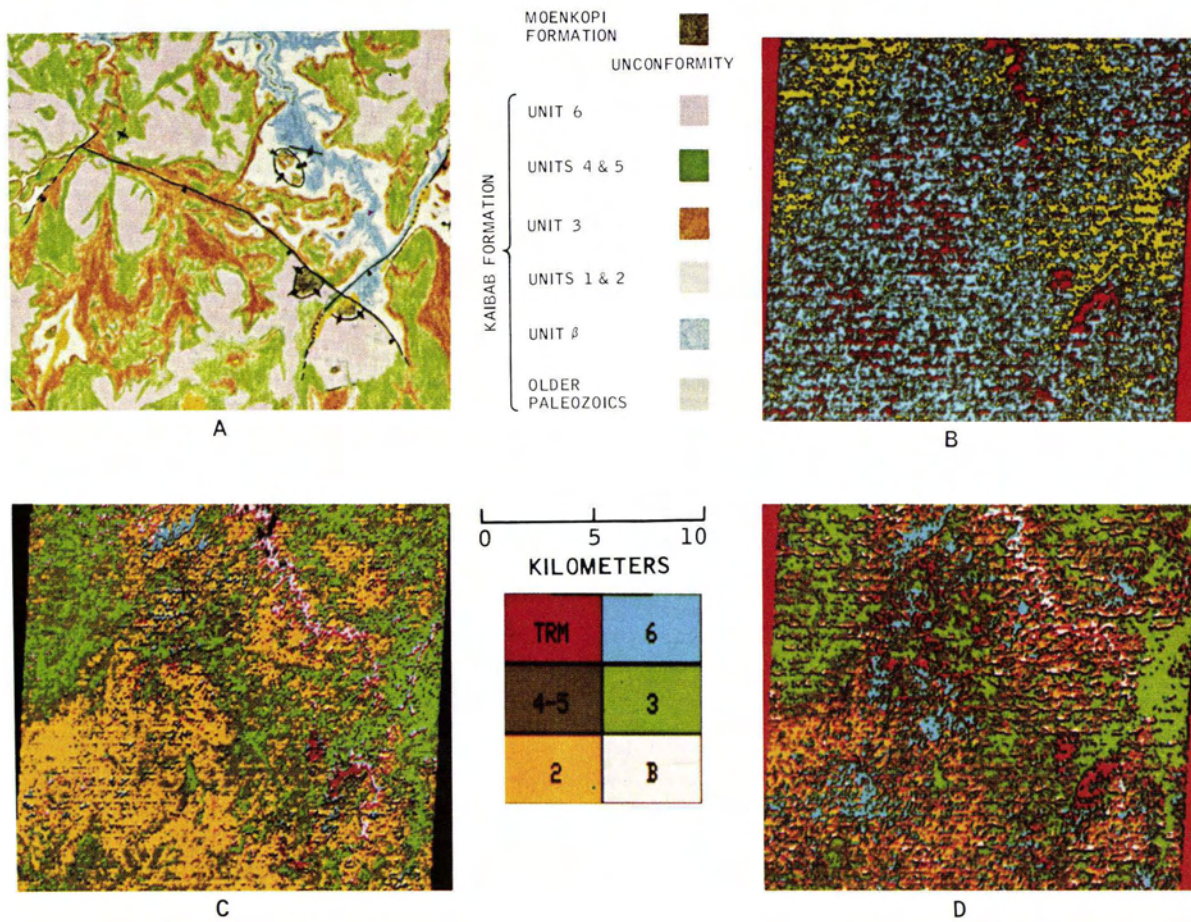| TRM	6
4-5	3
2	B

C

D

PLATE 1.   Study area in the Coconino Plateau, Arizona. (A) Detailed geologic map. (B) Classification map using an unsupervised (CLUS) algorithm. (C) Classification map using a hybrid classifier which incorporates the Parallelepiped algorithm and the Bayesian maximum likelihood function. (D) Classification map using a linear discriminant analysis algorithm.
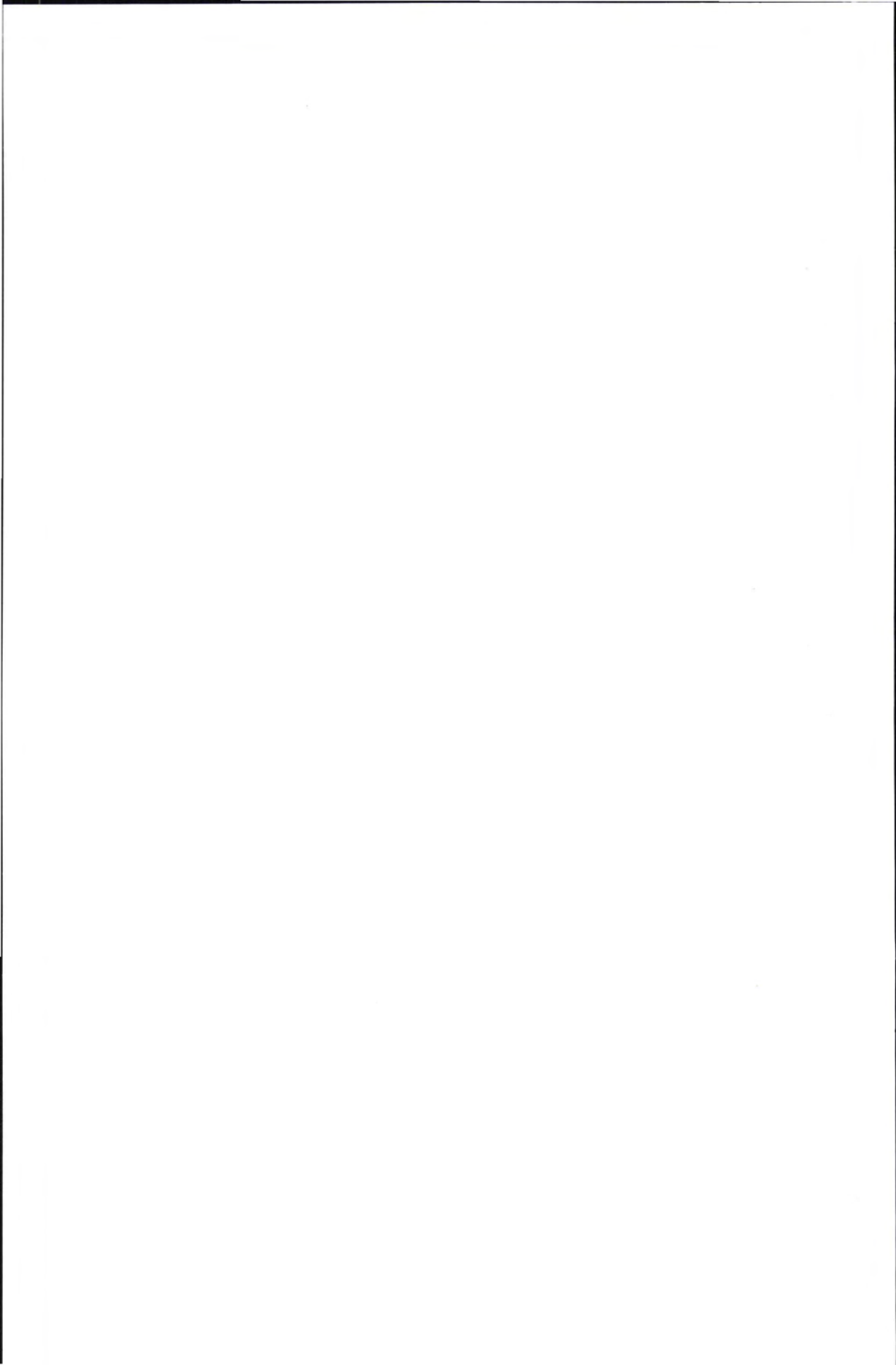
TABLE 3.   PARTITIONING CRITERIA
UNSUPERVISED CLASSIFICATION.
$n = 361$

No. of Groups	Log $(|T|/|W|)$	Diff. (Log $|T|/|W|$)	D^2	Diff. (D^2)
1	0.00		0.00	
		1.05		1.86
2	1.05		1.86	
		0.86		2.43
3	1.91		4.29	
		0.74		0.23
4	2.65		4.52	
		0.53		1.97
5	3.18		6.49	
		0.40		1.68
6	3.58		8.17	
		0.20		0.61
7	3.78		8.78	

number of 3 groups. A second maximum in the Mahalanobis D^2 criterion occurs between 4 and 5 groups.

A graphical illustration of the 3-group classification is presented in Figure 2 using discriminant functions 1 and 2 as the coordinates of the graph. As illustrated, the split between the three groups, A, B, and C, is almost entirely along discriminant function 1; over 91 per cent of the separability of the groups occurs along this function.

The five group classification was similar to the three group classification. In general, the members of group A in the three group classification were split into two groups. Four individual pixels, originally members of group C in the three group classification, comprised the fifth group.
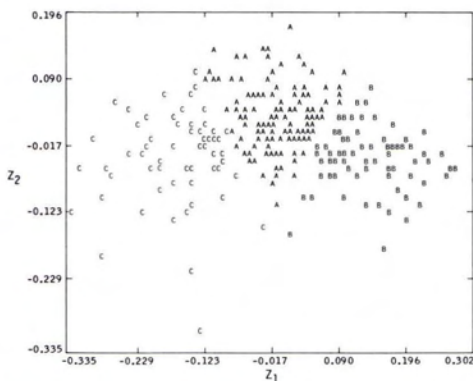

FIG. 2.   Plot of the 361 pixels partitioned into three groups. The coordinates of the graph, Z_1 and Z_2, are the first and second discriminant functions, respectively. A, B, and C represent one or more pixels in their respective groups.

The multiple discriminant functions computed from CLUS for the three and five group classifications were used to classify all the pixels within the study region. The results for the three group classification are shown in Plate 1b; the five group classification picture was not significantly different. Using an IBM 360/44 computer, the three group classification required 2-1/4 minutes for the entire study area.

SUPERVISED CLASSIFICATION

Hybrid Classifier. As a preliminary step in using the hybrid classifier algorithm, the four MSS bands and six ratios were analyzed to determine the minimum number of inputs necessary to separate the themes. For each of the ten variables, the means $(\overline{X}_i)$ and standard deviations $(\hat{\sigma}_i)$ of the themes were computed. The themes were compared pairwise for each variable, and were deemed separable if

$$\frac{\overline{X}_1 - \overline{X}_2}{c(\hat{\sigma}_1 + \hat{\sigma}_2)} > 1$$

where c is a specifiable weighting factor. The best separability of the six themes required the use of six variables, bands 4, 5, 7 and ratios 4/5, 4/6 and 4/7.

These variables and the associated statistics of themes were passed on to the hybrid classifier, and the study area was classified. The result is shown in picture form in Plate 1c. In order to classify the 63,516 pixels of the study area the Bayesian algorithm was called 59,429 times; a total of 6-1/2 minutes of Computer Processing Unit (CPU) time was required.

Discriminant Analysis. The ten variable data set for each theme was analyzed according to the linear discriminant algorithm presented previously. On the basis of the F-statistics and the improvement in the classification of each of the themes, as indicated by the classification matrix computed from the discriminant analysis algorithm (see Analysis of Results section), three variables, MSS bands 4, 5 and ratio 4/5, were used to compute the classification functions.

The unknown pixels within the study area were classified into one of the specified themes by computing their classification function for each of the themes and assigning them to the class for which they had the largest classification function. The results are shown in picture form in Plate 1d. Two minutes of CPU time were required for the classification.

CLASSIFICATION RESULTS

The thematic maps produced by the unsupervised classification algorithm (CLUS) and the two supervised classification schemes, the hybrid algorithm, and the linear discriminant analysis algorithm, were overlaid on the geologic map (see Plate 1a) and areas correctly and incorrectly classified were identified.

Both supervised classification schemes correctly classified approximately half of the study region. By using the discriminant classification algorithm, all outcrops of the Moenkopi Formation were correctly identified; however, an equal area was incorrectly assigned to this unit. By using the hybrid classifier, all outcrops of Moenkopi were correctly identified; misclassification was minor.

Unit 6 was more accurately mapped by the discriminant analysis classifier, and approximately one-third of the outcrop areas was correctly classified; however, about one-tenth of the remaining study area was incorrectly classified as unit 6. Approximately 5 per cent of this unit was correctly classified by the hybrid algorithm, with only minor misclassifications.

Units 3 and 4-5 taken together were equally well mapped by both classification programs; approximately half of the outcrop area was correctly mapped. The hybrid classifier misidentified a greater per cent of the study area than the discriminant algorithm.

Approximately 40 per cent of unit 2 outcrop was correctly classified by the hybrid scheme and an equal area was misclassified. The discriminant analysis algorithm correctly recognized only half as much area as the hybrid classifier and also misclassified approximately half as much as the hybrid classifier.

The hybrid classifier correctly identified about half of the Beta unit; only a third of the unit was correctly identified by the other algorithm. Both misclassified an insignificant portion of the study area.

By using the unsupervised three group classification (see Plate 1b) many lithologic boundaries were correctly delineated, though identification of units was not accurate. Blue areas on Plate 1b correspond to outcrop areas of units 6, 2, and some of units 3, and 4-5. Red areas include all outcrops of the Moenkopi Formation, some of the Beta outcrops along Cataract Creek, and miscellaneous areas of the other geologic units. The green areas are, in general, outcrops of units 3 and 4-5. It is not possible to determine the per cent of the area correctly classified, when classifying six geologic units into three groups.

ANALYSIS OF RESULTS

Two important considerations in choosing an automated classification algorithm are computational time and accuracy. In this study, the preliminary processing of the data for both supervised classification algorithms required approximately 30 seconds of CPU time on an IBM 360/44 computer. However, classification of the 63,516-pixel area study was three times as fast using the linear discriminant analysis algorithm (2 minutes vs. 6-1/2 minutes of CPU time) and required fewer inputs than the hybrid approach. The hybrid approach, nevertheless, is more efficient than classification schemes such as Purdue University's LARSYS, which computes the maximum likelihood function for every pixel for every class.

The unsupervised iterative partitioning of the grid data using the CLUS algorithm for 2 through 7 groups required 30 minutes of CPU time. By using the discriminant functions computed from CLUS for the three group classification, the study area was classified in two minutes of CPU time.

In terms of accuracy, both of the supervised classification schemes were comparable though they correctly classified only 50 per cent of the study area. The unsupervised algorithm delineated the major lithologic boundaries and, in a very general way, delineated each of the lithologic units.

The Beta unit and the Moenkopi Formation were most accurately mapped by all three algorithms. Identification of the other

units was not so successful. There appear to be several reasons for this lack of success. Facies changes of geologic units are prevalent but not generally recognized in delineating mappable units for regional mapping. This was not a serious problem in the study region because changes were slight and consisted of an increase or decrease in the siltstone/sandstone composition of the clastic units. Vegetation cover can pose a very important problem in lithologic identification. In the study area, vegetation cover is minimal. Vegetation communities were constant for any one lithologic unit, and the only significant change observed was associated with the change from one lithology to another. Problems of alluvial outwash masking or covering the bedrock is a significant factor affecting comparison of LANDSAT-derived classification maps with geologic maps. Because a geologic map represents bedrock geology without soil cover, it is an idealization of the true physical setting. LANDSAT senses only the surface of the ground, it does not penetrate through the soil mantle. In some instances, transported surface material may be derived from different lithology, unrelated to the underlying bedrock. Another effect of this transport phenomenon is to obscure sharp lithologic boundaries and produce gradational boundaries.

The above factors contribute to producing inhomogeneity in the spectral signatures of the training areas. To assess the significance of this effect, the spectral homogeneity of the training areas was examined by use of the CLUS algorithm. Using four principal components for the ten variable data set of the training areas taken together, classification was performed for two through seven groups. Various options were used to improve the initial grouping. The results are tabulated in Table 4. As indicated, the geologic themes are not spectrally homogeneous for the range of groups tested, i.e., the variation within groups is greater than the variation between groups.

A second major reason for the inability of the classification schemes to discriminate the geologic themes is the similarity of their spectral signatures in the four LANDSAT bands. (See Figure 3).

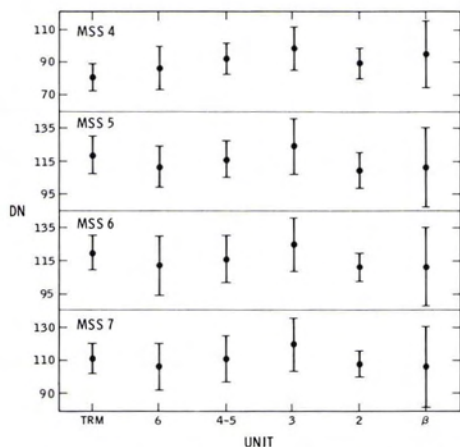There are two possible solutions to this problem. First, increase the sample size for

FIG. 3. Mean and two standard deviation plots of the spectral reflectivity of the geologic units from LANDSAT data.

TABLE 4. UNSUPERVISED CLASSIFICATION OF THEMES (A = TRM; B = UNIT 6; C = UNIT 4-5; D = UNIT 3; E = UNIT 2; F = UNIT β)

NUMBER OF GROUPS	1	2	3	4	5	6	7
2	25A						
	31B	19B					
	23C	27C					
	3D	47D					
	27E	23E					
	21F	49F					
3	7A		18A				
	17B	5B	23B				
	23C	9C	18C				
	22D	26D	2D				
	22E	9E	19E				
	14F	23F	13F				
4	2A			23A			
	16B	6B		23B			
	22C	10C		18C			
	25D	25D					
	21E	12E		17E			
	10F	25F	9F	6F			
5		10A	3A	12A			
		16B	14B	17B	3B		
	4C	10C	13C	16C	11C		
	12D	9D	8D	8D	25D		
	3E	14E	13E	13E	7E		
	20F	3F	16F	6F	5F		
6		11A	2A	11A	1A		
		17B	14B	16B	3B		
		10C	12C	18C	6C	4C	
		9D	9D	8D	12D	12D	
		14E	12E	14E	7E	3E	
	9F	3F	16F	6F	4F	12F	
7		7A	4A	8A	2A		4A
	3B	16B	10B	10B	5B	2B	7B
	6C	6C	3C	14C	14C	1C	6C
	5D	7D	5D	1D	17D	10D	5D
	12E	12E	7E	7E	5E		7E
	1F	6F	11F	5F	5F	12F	10F

GROUP NUMBER

each theme—this is difficult to do unless the study area is very well known (in which case there is no need for classification). Second, examine the spectral reflectance in wavelength bands different from LANDSAT to determine if greater lithologic separation is possible.

To evaluate the second solution, reflectance spectra of representative samples of the five geologic themes were acquired in the field by use of a portable reflectance spectrometer (Goetz et al., 1975). Reflectance was measured continuously over the range of 0.45 to 2.4 μm, which includes the 0.5 to 1.1 μm region scanned by LANDSAT. The spectra were digitized at 0.05 μm intervals in the region of 0.4 to 1.0 μm and at 0.1 μm intervals thereafter. A total of 83 spectra were analyzed. Using the stepwise linear discriminant analysis algorithm, the four best wavelengths for separability of themes were determined. They are, in order of separability, 1.3 μm, 1.0 μm, 0.5 μm, and 1.2 μm. On the basis of the optimum linear combination of these bands, the probability of each sample coming from each of the themes was computed, and the samples were assigned to the theme for which their probability was the greatest. The classification matrix is presented in Table 5. The classification is much better than that obtained by using the LANDSAT bands, and only unit 3 is not, in general, classified correctly. If the spectral reflectivity of the samples measured in the field is representative of the geologic units, then greater discrimination of rock type could be obtained by use of wavelength bands outside the region of LANDSAT.

SUMMARY AND CONCLUSION

Three different classification algorithms were applied to the problem of automated lithologic mapping of LANDSAT MSS data. The two supervised classification algorithms analyzed, the linear discriminant analysis algorithm and the hybrid algorithm which incorporated the Parallelepiped algorithm

and the Bayesian maximum likelihood function, were comparable in terms of accuracy, although both correctly classified only 50 per cent of the study region. The unsupervised classification algorithm which incorporated the CLUS procedure delineated some of the major lithologic boundaries but classification accuracy was far less than the supervised schemes.

The inability of the various classification schemes to portray correctly the lithologic units recognized in the field reflects the effects of spectral inhomogeneity of geologic units and the similarity of their spectral signatures in the LANDSAT bands.

More accurate lithologic classification may be possible by using spectral reflectance data from a wider wavelength region than that sensed by LANDSAT.

REFERENCES

Addington, J. (1975), A Hybrid Classifier Using the Parallelepiped and Bayesian Techniques, in Proc. of Amer. Soc. of Photogrammetry, 41st Annual Mtg., March 9-14, 1975, Washington, D. C., pp. 772-784.

Anderson J. R., E. E. Hardy, and J. T. Roach (1972), A Land Use Classification System for Use with Remote Sensor Data, USGS Circular 671, USGS, Washington, D. C., p. 16.

Bauer, M. E., and J. E. Cipra (1973), Identification of Agricultural Crops by Computer Processing of ERTS MSS Data, in Proc. of the Sympos. on Significant Results Obtained from ERTS-1, NASA/GSFC, Greenbelt, MD., March 5-9, 1973, Vol. 1, Sect. A., pp. 205-212.

Block, F. (1972). A Multivariate Chemical Classification of Rocks from the Montregian Petrographic Province, Quebec, Canada, Unpubl. Ph.D. Thesis, Dept. of Geosciences, The Pennsylvania State University, University Park, PA, p. 172.

Cooley, W. W., and P. R. Lohnes (1962), Multivariate Procedures for the Behavioral Sciences, John Wiley and Sons, Inc., p. 211.

Draeger, W. C., J. D. Nichols, A. S. Benson, D. G. Larrabee, W. M. Senkus, and C. M. Hay (1973), Regional Agricultural Surveys Using ERTS-1 Data, in Proc. of the Sympos. on Sig-

TABLE 5.   CLASSIFICATION MATRIX
NUMBER OF CASES CLASSIFIED INTO GROUP

Group	Trm	Unit 6	Unit 4-5	Unit 3	Unit 2
Trm	19	0	0	1	0
Unit 6	0	14	0	1	0
Unit 4-5	0	0	14	3	3
Unit 3	0	4	3	5	0
Unit 2	0	0	5	0	13

nificant Results Obtained from ERTS-1, NASA/GSFC, Greenbelt, MD, March 5-9, 1973, Vol. 1, Sect. A., pp. 117-126.

Ellefsen, R., P. H. Swain, and J. R. Wray (1973), Urban Land Use Mapping by Machine Processing of ERTS-1 Multispectral Data: A San Francisco Example, in *Proc. of Conf. on Machine Processing of Remotely Sensed Data*, Laboratory for Applications of Remote Sensing, Purdue University, W. Lafayette, Ind., Oct. 16-18, 1973, P2A-7-2A-22.

Goetz, A. F. H., F. C. Billingsley, D. P. Elston, I. Lucchitta, E. M. Shoemaker, M. J. Abrams, A. R. Gillespie, and R. L. Squires (1975), *Application of ERTS Images and Image Processing to Regional Geologic Problems and Geologic Mapping in Northern Arizona*, Jet Propulsion Laboratory Technical Report #32-1597, pp. 188.

Griffiths, J. C. (1968), Geological Data for Classification, in *Proc. of a Sympos. on Decision Making in Mineral Exploration*, Vancouver, Canada. Reprinted in *Western Miner*, Feb. and April 1968: Contribution No. 67-37, College of Earth and Mineral Sciences, The Pennsylvania State University, University Park, PA.

Griffiths, J. C. (1970), Aspects of Classification, in R. Protz and I. P. Martini (eds.), Classification of Soils and Sedimentary Rocks, in *Proc. of Symposium held at the University of Guelph*, Dept. of Resource Science, Published by University of Guelph, pp. 123-146.

Hempel, C. G. (1952), Fundamentals of Concept Formation in Empirical Science, Vol. 1-11 of the *International Encyclopedia of Unified Science*, University of Chicago Press, Chicago, pp. 93.

Imbrie, J. and E. G. Purdy (1962), Classification of Modern Behamian Carbonate Sediments, in W. E. Ham (ed.), *Classification of Carbonate Rocks, A Symposium:* Memoir 1, Amer. Assoc. Petroleum Geologist, pp. 253-272.

Landgrebe, D. and Staff (1973), An evaluation of Machine Processing Techniques of ERTS-1 Data for User Applications, in *Proc. of the Sympos. on Significant Results Obtained from ERTS-1*, NASA/GSFC, Greenbelt, MD, December 10-14, 1973, Vol. 1, Sect. A., pp. 41-73.

Melhorn W. N. and S. Sinnock (1973), Recognition of Surface Lithologic and Topographic Patterns in Southwest Colorado with ADP Techniques, in *Proc. of the Sympos. on Significant Results Obtained from ERTS-1*, NASA/GSFC, Greenbelt, MD, March 5-7, 1973, Vol. 1, Sect. A., pp. 473-481.

Rowan, L. C., P. H. Wetlaufer, A. F. H. Goetz, F. C. Billingsley, and J. H. Stewart (1974), *Discrimination of Rock Types and Detection of Hydrothermally Altered Areas in South-Central Nevada by the Use of Computer-Enhanced ERTS Images*, Geol. Survey Prof. Paper #883, 35 p.

Rubin, J. and H. P. Friedman (1967), *A Cluster Analysis and Taxonomy System for Grouping and Classifying Data*, I.B.M. Corporation, New York Scientific Center, 590 Madison Avenue, New York, NY 10022, p. 221.

Siegal, B. S. and J. C. Griffiths (1975), *Classification of Glacial Tills by Computer—Using the CLUS Program*, Computers and Geoscience, Vol. 1, No. 1, No. 1/2, pp. 65-74.

Wigton, W. H. and D. H. Von Steen (1973), Crop Identification and Acreage Measurement Utilizing ERTS Imagery, in *Proc. of the Sympos. on Significant Results Obtained from ERTS-1*, NASA/GSFC, Greenbelt, MD, March 5-9, 1973, Vol. 1, Sect. A., pp. 87-92.